

Conf 781033--13

**MASTER**

LA-UR-78-2755

**TITLE:** BIOMEDICAL APPLICATIONS OF MEDIUM ENERGY PARTICLE BEAMS AT LAMPF

**AUTHOR(S):** James N. Bradbury

**SUBMITTED TO:** Proceedings of the IEEE Nuclear Science Symposium, Washington, D.C., October 1978.

**NOTICE**

This report was prepared as an account of work sponsored by the United States Government. It is hereby stated that the United States Government is authorized to reproduce and distribute reprints for government purposes not withstanding any copyright notation that may appear hereon. It is understood that any copyright in any process in connection with this report, if any, shall be owned by the individual(s) named in this report.

By acceptance of this article for publication, the publisher recognizes the Government's (license) rights in any copyright and the Government and its authorized representatives have unrestricted right to reproduce in whole or in part said article under any copyright secured by the publisher.

The Los Alamos Scientific Laboratory requests that the publisher identify this article as work performed under the auspices of the USERDA.



**Los Alamos  
scientific laboratory**  
of the University of California  
LOS ALAMOS, NEW MEXICO 87544

An Affirmative Action/Equal Opportunity Employer

28  
REVISED

BIOMEDICAL APPLICATIONS OF MEDIUM ENERGY  
PARTICLE BEAMS AT LAMPF\*

James N. Bradbury†

Abstract

At LAMPF an 800-MeV proton accelerator is used to produce intense beams of secondary protons, pi mesons, and muons which are being employed in several areas of biomedical research. The primary proton beam is used to produce short-lived radioisotopes of clinical interest. Carefully tailored secondary proton beams are used to obtain density reconstructions of samples with a dose much less than that required by x-ray CT scanners. The elemental composition of tissue samples is being determined non-destructively with muonic x-ray analysis. Finally, an extensive program, with physical, biological, and clinical components, is underway to evaluate negative pi mesons for use in cancer radiotherapy. The techniques used in these experiments and recent results are described.

Introduction

At the Clinton P. Anderson Meson Physics Facility (LAMPF) a linear accelerator is used to generate intense beams of 800-MeV protons. These protons, interacting with appropriate targets, produce copious fluxes of secondary protons, neutrons, pi mesons (pions), and muons which can be delivered to a number of different

experimental areas shown in Fig. 1. LAMPF is a national facility, open to all qualified researchers, and is presently providing a proton current of 500  $\mu$ A with the design goal of 1 mA expected in 1980.

The basic research program at LAMPF involves experiments in nuclear physics, medium energy particle physics, nuclear chemistry, and solid-state physics. Largely as a result of the high beam intensities, an extensive applied research program is also underway which includes materials analysis investigations with protons, muons, and neutrons; radiation damage studies with protons and neutrons; radioisotope production with protons; and cancer radiotherapy with negative pions. Accelerator technology is also being transferred to biomedicine through the use of localized rf current fields to produce hyperthermia for the treatment of tumors. In this paper the subset of applied research at LAMPF aimed at biomedical applications is discussed.

Radioisotope Production

The primary proton beam passes through three pion production targets and about 50% of the original current is available for radioisotope production at the beam stop area.<sup>1</sup> Up to nine stringers can be remotely

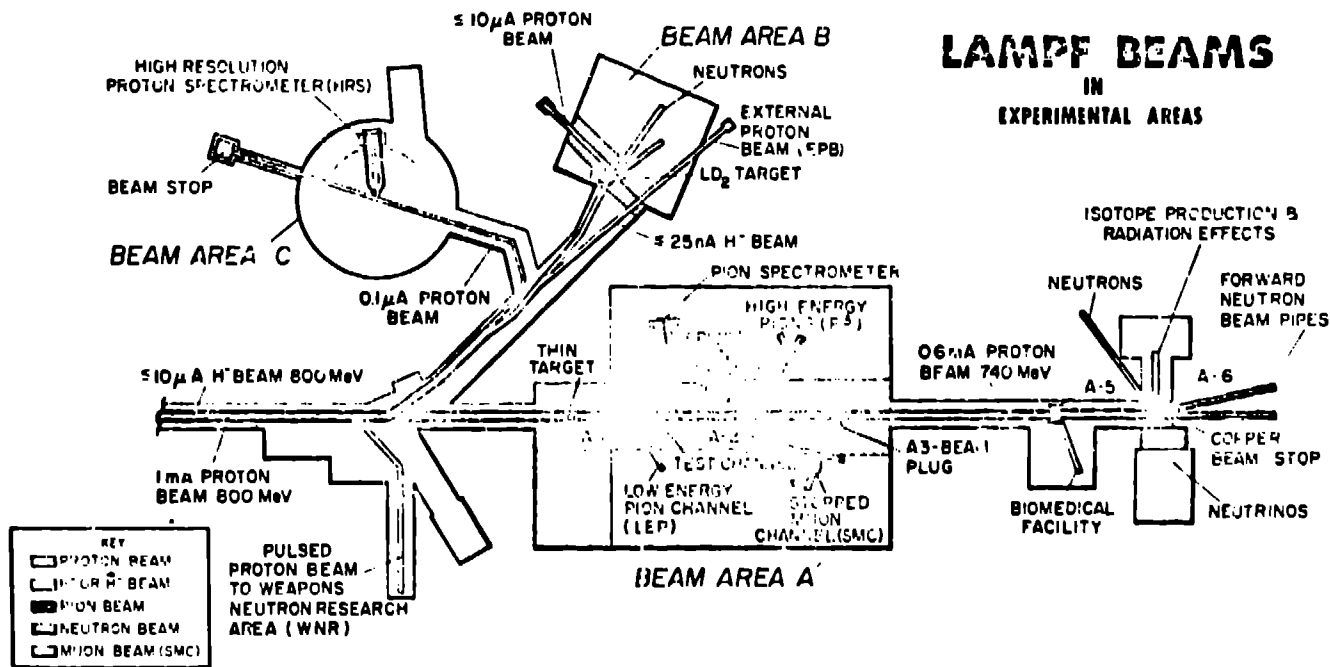


Fig. 1 Experimental areas at LAMPF. Area A is used primarily for meson physics, Area B for neutron physics and nuclear chemistry, and Area C for nuclear physics.

\*This work was supported by the U.S. Department of Energy.

†University of California, Los Alamos Scientific Laboratory, Los Alamos, NM 87545.

inserted into and retracted from the beam line; each stringer can contain a 2.5-cm-thick, water-cooled target in which radioisotopes are produced through proton-induced spallation processes. After appropriate irradiation times the targets are placed in shielded casks and transported to another LASL laboratory for isotope separation and purification by radiochemical techniques. Most LAMPF radioisotopes are on the proton-rich side of stability and have short lifetimes and/or low production cross sections to capitalize on the high proton beam intensity. Those medical isotopes which are either undergoing development or are now in production and being delivered to various research institutions, are listed in Table 1.

Table 1

LAMPF Radioisotopes

Target	Product	Use
Mo	$^{82}\text{Sr} \rightarrow ^{82}\text{Ru}(75\text{s})$	Blood dynamics studies
Mo	$^{77}\text{Br}(56\text{h})$	Pharmaceutical labeling
La	$^{127}\text{Xe}(36\text{d})$	Pulmonary studies
La	$^{123}\text{Xe} \rightarrow ^{123}\text{I}(13\text{h})$	Thyroid imaging
V	$^{44}\text{Ti} \rightarrow ^{44}\text{Sc}(4\text{h})$	Bone scanning agent
Ni	$^{52}\text{Fe}(8\text{h})$	Brain scanning agent

Proton Computed Tomography

In this technique a nearly monochromatic beam of protons is passed through a sample, and the residual energy of individual exiting protons is precisely measured with a solid-state detector or range telescope, which provides a measure of the integrated density along the beam path. If the beam is passed through the sample from a number of different directions the density distribution within the sample may be reconstructed, using computer algorithms, in a manner analogous to that employed in commercial x-ray CT scanners which are being widely used to detect and localize internal abnormalities like tumors. It is expected on theoretical grounds that scans with charged particles like protons should require substantially less dose than x-ray scans to achieve a given density resolution.

At LAMPF a channel was tuned to provide a spatially collimated secondary beam of protons with an energy of 200 MeV and an energy spread of 0.4%. A proton computed tomography experiment was carried out using the arrangement shown in Fig. 2.<sup>2</sup> A phantom, with inhomogeneities designed to provide quantitative determination of spatial and density resolution, was immersed in a water bath to limit the required dynamic range and placed in the proton beam. The residual energy of the protons was measured with a hyperpure Ge detector, and a multiwire proportional counter was used to measure the proton exit position so that a correction for multiple scattering could be applied. Tests indicated that a density resolution of less than .01% could be obtained. The phantom was translated and rotated to provide a large number of views, and the density distribution was reconstructed using the energy and position measurements on some  $6 \times 10^7$  protons. The reconstruction is shown in Fig. 3. Subsequently, the phantom was scanned with a commercial x-ray scanner; the proton dose was a factor of about five less than the x-ray dose for a similar reconstructed density resolution (0.4% for 1 cm object). Future experiments using fixed and fresh human tissue specimens and high data acquisition rates will be aimed at determining whether, in addition to the dose advantage, protons also provide a contrast advantage

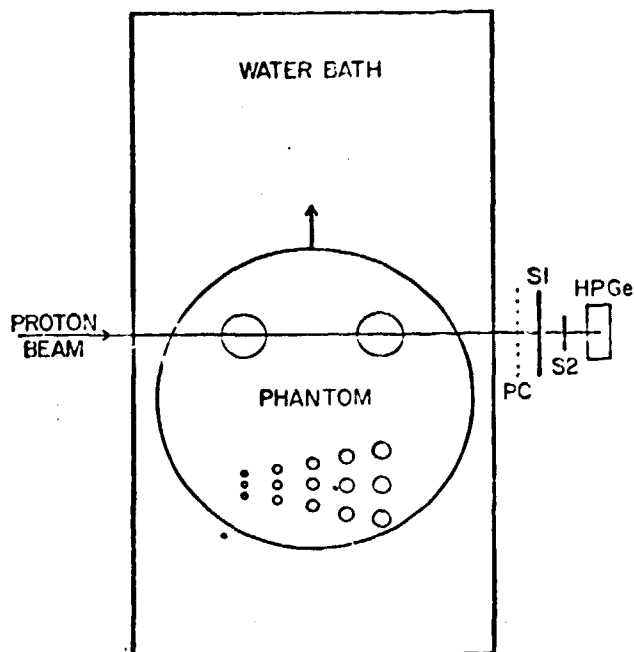


Fig. 2 The experiment arrangement for evaluating proton computed tomography including test phantom, proportional chamber to determine proton exit position, scintillators to trigger data acquisition system, and proton energy detector.

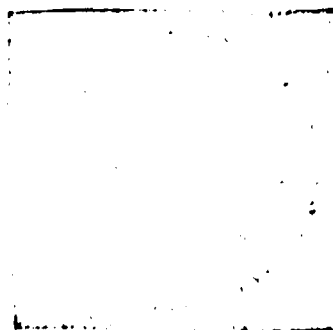


Fig. 3 Proton computed tomographic reconstruction of a 20-cm-dia test phantom; the smallest holes are 3 mm in diameter and density variations are less than 2%.

over x rays as a result of the different energy loss mechanisms involved.

Muonic X-Ray Analysis

LAMPF has a channel which is designed to provide intense beams of energetic muons, the decay products of pions. When negative muons are implanted in a sample, they slow to an energy of a few eV and are captured by a nucleus to form a muonic atom. The muon cascades down to more tightly bound orbits in the atom emitting x rays whose energies are characteristic of the capturing element as is the case with electron transitions. The entire process occurs in a time short compared to the muon lifetime of  $2 \times 10^{-6}$  s. Since the mass of the muon is about 200 times that of the electron, the x rays are much more energetic than electronic characteristic x rays; muonic x rays easily escape bulk samples with low absorption and may be detected with good efficiency by Ge(Li) detectors. In a mixture of elements the probability of muon capture as a function of atomic number

can be empirically determined (and approximately predicted theoretically) so analysis of the intensities and energies of the x rays provides a quantitative determination of the elemental composition of the sample. Muonic x-ray analysis is non-destructive and, although not suitable for trace element analysis, the technique can be used to detect elements in concentrations down to about the 0.1% level. Also the intensities of large samples can be interrogated, and some selectivity can be achieved by varying the muon energy and thus the stopping region. Finally, in contrast to most conventional analytical techniques, muonic x-ray analysis can be used to detect all elements with atomic numbers greater than two; in particular, it can be applied to analyses of bulk samples of organic materials whose primary constituents are low-Z elements.

A number of samples of biological and environmental interest have been analyzed with muons at LAMPF, including human tissues and organs,<sup>3</sup> coal samples, and reactor fuel rod materials. In Fig. 4 the muonic x-ray spectrum from a normal human liver sample is shown with lines from C, N and O. A similar spectrum obtained from a cirrhotic liver has been analyzed to reveal about a 6% difference in the oxygen to carbon ratio, reflecting a larger fat concentration. This suggests the possibility of using muonic x-ray analyses for the *in vivo* diagnosis of diseases which give rise to abnormal concentrations of elements such as hemochromatosis, cirrhosis, osteoporosis, and perhaps some types of cancer. An experiment will be performed soon to ascertain the utility of the technique in monitoring the concentration of calcium in bone in patients undergoing drug therapy.

Recent experiments have shown that the chemical structure of the environment in which the stopping muon finds itself influences the intensities of the x-ray lines within a series.<sup>4</sup> This feature may ultimately prove to be the greatest advantage of the muonic x-ray analysis technique. The atomic valence electrons, which are involved in the chemical bond of a compound, apparently affect the angular momentum of the very slowly moving muon and hence the details of the muon cascade. For example, in hydrocarbons, higher H:C ratios are accompanied by higher Lyman  $\beta$  to Lyman  $\alpha$  ratios indicating muon capture into lower angular momentum states. Thus analysis of intensities can provide information on chemical bond configurations and strengths. When such chemical effects on capture are better understood, the muonic x-ray analysis technique may become a unique tool for the simultaneous investigation of elemental composition and chemical structure in biological materials.

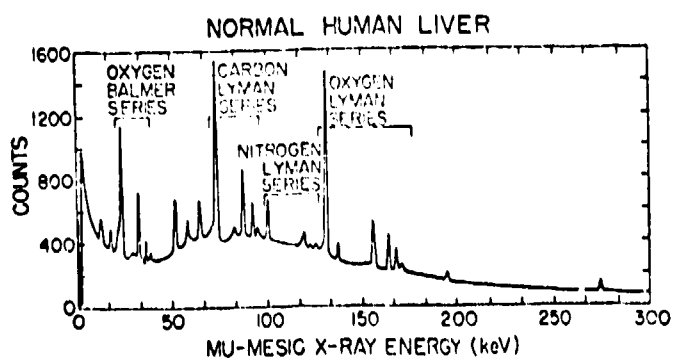


Fig. 4 Muonic x-ray spectrum from a frozen human liver sample. The intensities of the x-ray lines can be used to determine the element concentrations.

### Cancer Radiotherapy with Negative Pions

Each year about 400,000 people in the United States receive x-ray or  $\gamma$ -ray radiation as a major or supporting part of cancer therapy. Improvements in radiotherapy could benefit some 60,000 people annually who die because of lack of tumor control at the primary site; many additional patients with metastasized disease may also be helped since any large reduction in the body's total burden of tumor cells improves the chances for cure by conventional techniques. Conventional radiotherapy failures are often due to an inability to deliver a lethal dose to the tumor, which may be radioresistant, with acceptable normal tissue damage. To increase cure rates through radiotherapy, it is necessary to achieve improved dose localization and/or improve the quality of radiation to help overcome tumor radioresistance. One or both of these improvements are possible with particles such as pions, neutrons, protons, and heavy ions, all of which are currently being evaluated for use on those types of large tumors which are not well managed by x rays, surgery, and drugs, alone or in combination.

### Advantages of Pions

Pions, like other charged particles, have a definite, adjustable range in matter and deposit most of their energy near the end of that range thus providing localization of dose. In contrast, x rays,  $\gamma$  rays, and neutrons have exponential depth-dose curves leading to significant deposit of dose in the entrance and exit regions surrounding the tumor volume. A second advantage of negative pions compared to conventional radiations lies in their "strong-interaction" character which is responsible for the binding of nucleons together in nuclei. When a negative pion comes to rest, it is captured by a tissue nucleus; the pion-nucleus interaction results in the liberation of the pion rest-energy of 140 MeV causing the nucleus to undergo fragmentation. The heavier fragments, have short ranges and are densely ionizing on a microscopic scale. Such particles are said to provide high linear energy transfer (LET) if they deposit more than about 75 keV per micron. High-LET particles have a greater probability of creating double-strand breaks in DNA molecules, which are difficult to repair and usually lead to cell inactivation than low-LET radiations such as x rays and protons. Approximately 5-15% of the dose in the pion stopping region is high-LET in character and hence is biologically more effective in overcoming tumor radioresistance due to lack of oxygen and also variations in cell-cycle sensitivity. Thus, in-flight pions behave as low-LET radiation as they are delivered to a tumor volume, sparing normal tissue to some extent; in the stopping region, however, which can be tailored to overlap the tumor volume, there is a significant component of high-LET radiation with enhanced biological effectiveness. Although the potential advantages of pions for radiotherapy have been realized for decades, evaluation of this modality has awaited the advent of meson factories to produce therapeutically useful dose rates.

### LAMPF Biomedical Facility

The program at LAMPF to evaluate negative pions for cancer therapy is jointly funded by the National Cancer Institute and the Department of Energy, and jointly carried out by LAMPF and University of New Mexico staff. A dedicated biomedical facility, shown in Fig. 5, is used to conduct the necessary physics and radiobiology research and the clinical trials. The primary proton beam impinges upon an 8-cm carbon target generating pions which are collected and transported to the treatment room by a series of 11 magnets. The channel is designed to yield a pion beam with a small momentum

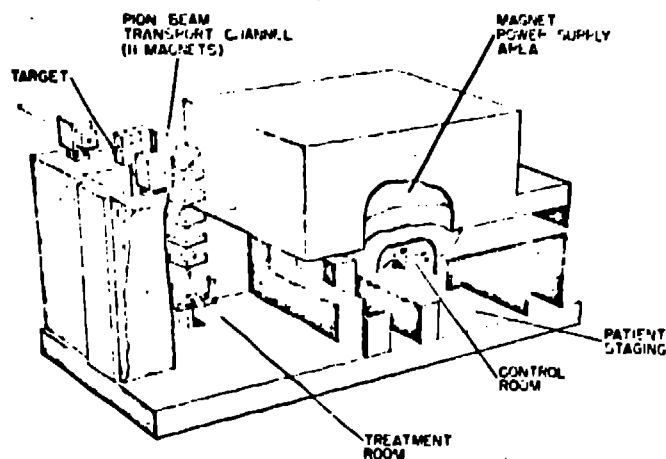


Fig. 5 The LAMPF biomedical facility. The complex contains a pion channel and treatment room, physics laboratories, radiobiology laboratories, and patient handling areas.

spread (which produces a narrow dose peak) in order to produce sharp edges in the dose distribution. To fill a large tumor volume, this narrow peak is spread in depth by a programmable, hydraulically actuated range-shifter.<sup>5</sup> The channel contains slits for beam definition and safety purposes, an ionization chamber for monitoring dose, and instrumentation for mapping the phase space of the particles. A computer is used to control and monitor all of the hardware in the pion delivery system, motion of the patient treatment couch, and the patient treatment itself.

#### Beam Development and Characterization

The magnets in the channel are tuned with multi-wire proportional chambers to shape pion beams of various sizes for therapy with the objective of maximizing dose rate and uniformity of dose in the field.<sup>6</sup> Time-of-flight techniques are used to measure the low LET electron and muon contamination flux which is typically about 20% of the pion flux. A catalog of beam tunes has been developed which, in conjunction with appropriate range shifter functions, provides channel parameters for producing stopping pion distributions in volumes ranging from  $3 \times 3 \times 3 \text{ cm}^3$  to  $17 \times 17 \times 17 \text{ cm}^3$  at three different energies corresponding to maximum penetration depths of 12, 18, and 26 cm.

The three-dimensional dose distributions for the various beams are measured in water and effects of collimators and inhomogeneities assessed.<sup>7</sup> Also, the relatively small dose outside the stopping region due to beam contaminants and neutrons from the capture process is measured for different beams. Finally, microdosimetric measurements are made, using very thin Si(Li) detectors and thimble ionization chambers to determine quantitatively the LET distribution in the volume.<sup>8,9</sup> The high-LET component of the dose varies throughout the spread peak, depending upon the ratio of passing to stopping pions which produce the dose; the goal is to correlate LET measurements with radiobiology or clinical results to establish how to shape dose distributions to produce uniform biological effect. Several dose distributions are shown in Fig. 6; that labeled flat biological dose is tailored so that the increased high-LET dose in the downstream portion is compensated by a decreased physical dose. The dose

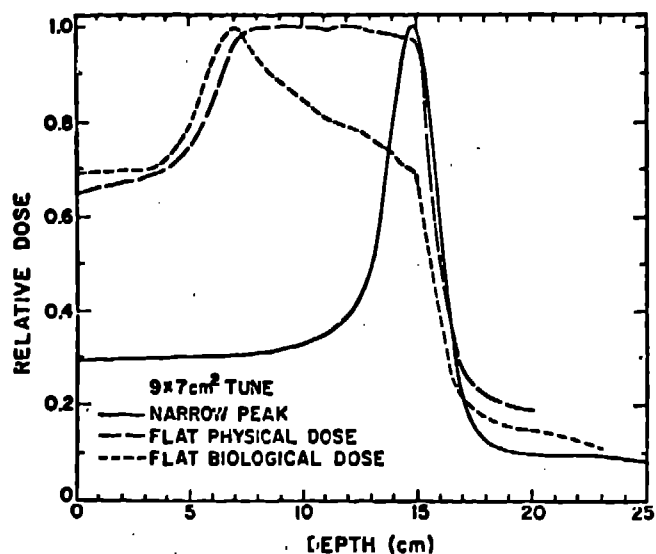


Fig. 6 Useful pion depth dose distributions for a medium energy tune with transverse dimensions  $9 \times 7 \text{ cm}^2$ , including narrow unmodulated peak and spread peaks. The range-shifted spread peaks can be arbitrarily tailored with respect to depth position, width, and slope to provide constant stopping pion distribution, flat physical dose, etc.

rate is approximately inversely proportional to the volume; the dose rate into a liter is about 10 rads/min with an accelerator proton current of  $500 \mu\text{A}$ . An example of the microdosimetry results showing the relative amounts of LET components is depicted in Fig. 7.

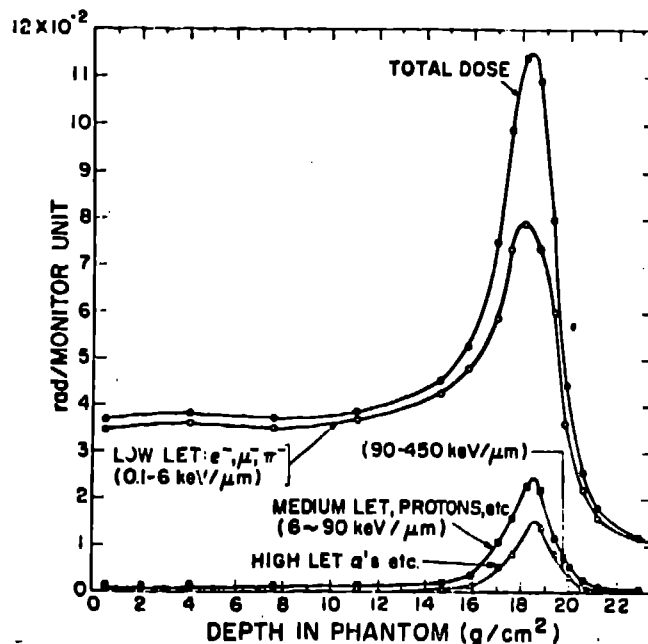


Fig. 7 Solid-state detector microdosimetry data showing the relative amounts of low and high LET components in the dose from an unmodulated beam.

## Radiobiology

The major aims of the radiobiology effort are 1) to study effects of pions on normal tissues using mouse lung, heart, kidney, etc. irradiations, to help guide the clinical trials, 2) to evaluate variation in biological effectiveness for different dose distributions using cell systems, mouse tumors, and multicellular tumor spheroids and 3) to investigate fundamentals of radiobiological action with mixed-field radiation. In a spread peak pions produce a biological effect ranging from about 20% to 60% greater than the x-ray control radiation and are about 10 to 25% more effective than x rays in overcoming intrinsic radioresistance due to hypoxia.<sup>10</sup> Recent experiments by Yuhas<sup>11</sup> in which x rays and pions are applied in a variable time sequence to cell systems seem to indicate that the mechanism of action for pions may involve the high-LET component of the dose inhibiting repair of sublethal injury caused by the low-LET component.

## Treatment Planning and Visualization

Computerized treatment planning is essential for delivering pions in an optimum manner to the unique tumor volume of a given patient. Each patient receives an x-ray computerized tomography (CT) scan which serves to determine both the location and extent of the tumor in the body and the integrated density between the patient surface and the tumor which is necessary for establishing the distribution of pion ranges required. On the basis of the CT scan a collimator is fabricated to limit the field in the transverse dimensions and a bolus is constructed to compensate for the patient inhomogeneities. The treatment planning code then transports the five-dimensional phase space characterizing the pions, muons, and electrons for an appropriate channel tune through the moving range shifter, collimator, and bolus and into the patient where the particles deposit dose in accordance with the detailed density distribution supplied by the CT scan. During the propagation of the particles the code takes into account multiple scattering, range straggling, pion and muon decay, and the high-LET dose resulting from pion capture. Isodose contours for different LET components can be calculated for evaluation by the physician. An example of a treatment plan for a pancreatic tumor utilizing parallel opposed overlapping ports is shown in Fig. 8.

A significant fraction of the pion captures results in gamma rays (from charge exchange and radiative capture processes, nuclear excitation, and residual radioactive nuclei) which escape the body. The trajectory of these gammas can be measured with collimators and detectors, thus determining the distribution of stopping pions. Experiments are underway to develop clinically useful instrumentation which will permit the stopping pion distribution to be visualized during patient treatment with a resolution of  $\leq 1$  cm. When referenced to the patient anatomy this will serve as a check on the treatment planning and the performance of the channel hardware. The experimental arrangement for visualizing gammas above about 10 MeV is shown in Fig. 9.

## Patient Treatments and Results

Patients are immobilized in casts and positioned by means of a crossed-beam laser system which is duplicated in the staging area and treatment room. The patient setup configuration is shown in Fig. 10. Parallel opposed overlapping ports are used where possible to optimize uniformity of distribution of both physical dose and high LET dose. Abutting fields are

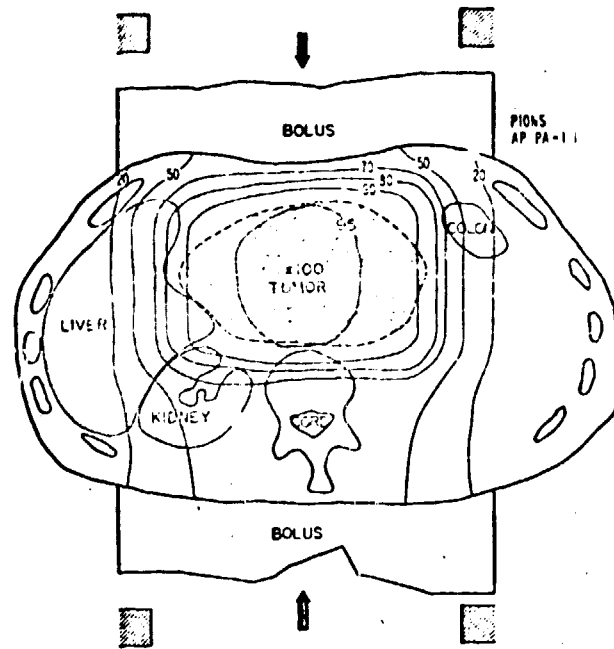


Fig. 8 Treatment plan using parallel opposed overlapping ports for a pancreatic tumor. The notch in the lower bolus compensates the pion energy for the spinal cord; large ports of critical organs receive considerably less dose than the tumor volume.

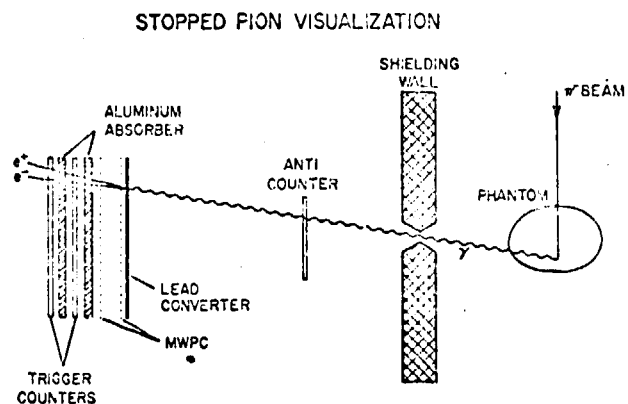


Fig. 9 Experimental arrangement using high-energy gammas to visualize the distribution of stopping pions. The gammas pass through a uranium collimator and, after conversion, are localized with a multiwire proportional counter. Trigger counters and absorber are used to set the gamma energy threshold.

used for treatments requiring a lateral dimension greater than 15 cm. For the treatments to date the pion beams ranged in energy from 60 to 110 MeV and the modulated pion peak was spread to dimensions up to 10 cm. As a check on treatment planning *in-vivo* dosimetry using TLD's and solid-state detectors has been performed on several patients with body cavities near the tumor volume. Static beams will be used for all treatments; very soon dynamic treatments will be initiated in which, under computer control, the patient is moved with respect to a spread fan-shaped beam while the range

## Clinical Pion Radiotherapy Patient Setup

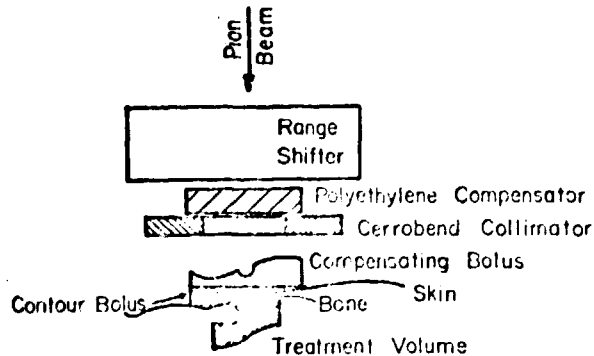


Fig. 10 The hardware configuration for a typical clinical pion radiotherapy patient setup.

shifter function is varied. This technique will improve dose localization since the depth distribution of the dose can be changed across the tumor volume.

As of October 1978 a total of 67 patients with 136 tumors have been treated with pions. Nine of these patients, with skin and subcutaneous metastases assigned randomly to pions and x rays, were treated early in the program, pions were shown to be 40% more effective than x rays in producing acute skin reaction. The measured time to regrowth of some nodules suggested the possibility of a therapeutic gain for pions versus x rays.<sup>12</sup>

Data on 40 patients with large advanced tumors treated with pions and followed from 6 to 15 months have been discussed by Kligerman et al.<sup>13</sup> Tumor sites included brain, head and neck, lung, breast, liver, abdomen, pelvis, and lymph nodes. In all cases it had been judged that conventional treatment modalities, alone or in combination, would not significantly benefit the patient. Total doses for each new tissue type were set low at the outset and were escalated with successive groups of patients as sufficient information was obtained to indicate that higher doses could be safely tolerated. The pion treatments were usually delivered in five fractions per week with daily fractions ranging between 110 and 140 peak pion rads requiring 10 - 15 minutes; total tumor doses ranged from 1000 to 4600 peak pion rads although most patients received less than 3300 rads. Some patients received conventional radiation or surgery subsequent to the pion treatment with no complications. Of the 40 tumors, 13 completely regressed, 16 partially regressed, and 11 exhibited no change. Complete regressions were observed only among those 21 tumors which received more than 2700 pion rads so for future treatments a minimum dose of 3300 rads has been established. Recent observations on patients treated with doses from 3300 to 4100 pion rads indicate that this dose range is close to normal tissue tolerance. Local recurrence after complete regression has been noted in only three patients. All 40 patients tolerated pion therapy well and, in general, acute reactions of normal tissues have been remarkably mild. There have been no serious untoward effects in any patient treated thus far.

## Medical Accelerators

Biomedical research is underway at LAMPF in several areas, including radioisotope production, computed tomography with protons, materials analysis with muons, and cancer therapy with negative pions. In the event that some or all of these applications of particles prove sufficiently worthwhile to warrant their widespread use, it is important to consider the practicality of dedicated accelerators. The design of a medical pion generator is being carried out at Los Alamos with emphasis on compactness, economy of construction and operation, and reliability.<sup>14</sup> A proton linear accelerator in the medium-energy class is envisioned using a 450-MHz drift-tube structure followed by a 1350-MHz disk and washer structure. The design features 250-keV injection energy, low duty factor, novel focusing techniques, and very high acceleration gradients. The use of a large solid angle pion collector would limit primary proton currents to less than 100  $\mu$ A. The accelerator length might be of the order of 120 m with a cost in the \$10-15 million range. The facility could be designed to accommodate radioisotope production, proton therapy, and proton tomography. (See Fig. 11.)

A dedicated pion medical facility would obviously be much more expensive than conventional radiotherapy equipment (which, of course, it would not supplant) but still represent a very small part of the \$30 billion annually spent on cancer care. A modest number of pion units, perhaps about 20, might be justified if pion therapy were able to save some 15% (9,000 patients) of those 60,000 patients who annually die of local disease. Since it is estimated<sup>15</sup> that each cure versus death represents a savings of about \$20,000, 9,000 additional cures would indicate an annual savings of \$180 million.

## References

1. H.A. O'Brien, Jr., A.E. Ogard, and P.M. Grant, "Radioisotopes from a Medium-Energy Accelerator: The Clinton P. Anderson Meson Physics Radioisotope Program," LA Report 74-1263.
2. K.M. Hanson, J.N. Bradbury, T.M. Cannon, R.L. Hutson, D.B. Laubacher, R. Macek, M.A. Paciotti, and C.A. Taylor, "The Application of Protons to Computed Tomography," IEEE Trans. Nucl. Sci. NS-25, 657-660 (1978).
3. R.L. Hutson, J.J. Reidy, K. Springer, H. Daniel, and H.B. Knowles, "Tissue Chemical Analysis with Muonic X-Rays," Radiology 120, 193-198 (1976).
4. J.D. Knight, C.J. Orth, M.E. Schillaci, R.A. Naumann, H. Daniel, K. Springer, and H.B. Knowles, "Chemical Effects in Negative Muon Capture in Some Ionic and Covalent Solids and Ionic Aqueous Solutions," Phys. Rev. A, 13, 43-53 (1976).
5. H.I. Amols, D.J. Liska, and J. Halbig, "The Use of a Dynamic Range-Shifter for Modifying the Depth Dose Distributions of Negative Pions," Med. Phys. 4, 404-407 (1977).
6. M. Paciotti, J. Bradbury, R. Hutson, E. Knapp, and O. Rivera, "Tuning the Beam Shaping Section at the LAMPF Biomedical Channel," IEEE Trans. Nucl. Sci. NS-24, 1058 (1977).

7. A.R. Smith, I. Rosen, K.R. Hogstrom, R.G. Lane, C.A. Kelsey, H.I. Amols, C. Richman, P.A. Berardo, J. Helland, R. Kittel, M. Paciotti, and J. Bradbury, "Dosimetry of Pion Therapy Beams," *Med. Phys.* 4, 409-413 (1977).
8. H.I. Amols, J.F. Dicello, T.F. Lane, F.W. Pfeufer, J.A. Helland, and H.B. Knowles, "Microdosimetry of Negative Pions at LAMPF," *Radiology* 116, 183-185 (1975).
9. C. Richman, "Characteristics of a Negative Pion Beam for the Irradiation of Superficial Nodules in Cancer Patients," *Rad. Res.* 66, 453-471 (1974).
10. M.R. Raju, H.I. Amols, E. Bain, S.G. Carpenter, J.F. Dicello, J. Frank, R.A. Tobey, and R.A. Walters, "Biological Effects of Negative Pions," *Int. J. Rad. Oncology, Biology and Physics*, 3, 334 (1977).
11. J. Yuhas, and A. Li, "Biological Effects of Negative Pi Mesons *in vitro*: Multicellular Tumor Spheroids," submitted to *Rad. Res.*
12. M.M. Kligerman, J.M. Sala, S. Wilson, and J.M. Yuhas, "Investigation of Pion Treated Human Skin Nodules for Therapeutic Gain," *Int. J. of Radiation Oncology, Biology, and Physics*, 4, 263-265 (1978).
13. M. Kligerman, S. Wilson, J. Sala, C. von Essen, H. Tsujii, J. Dembo, and M. Khan, "Results of Clinical Applications of Negative Pions at Los Alamos," in press, *Proceedings of the 3rd Meeting on Fundamental and Practical Aspects of the Application of Fast Neutrons and Other High LET Particles to Clinical Radiotherapy*, the Hague, The Netherlands, September, 1978, Pergamon Press, Oxford.
14. E.A. Knapp and D.A. Swenson, "The LASL Ion Linear Accelerator Program," *Int. J. Rad. Onc., Biol. and Phys.* 3, 383-385 (1977).
15. J.R. Stewart, J.A. Hicks, M.L.M. Boone, and L.D. Simpson, "Computed Tomography in Radiation Therapy," *Int. J. Rad. Onc. Biol. and Phys.* 4, 313-324 (1978).

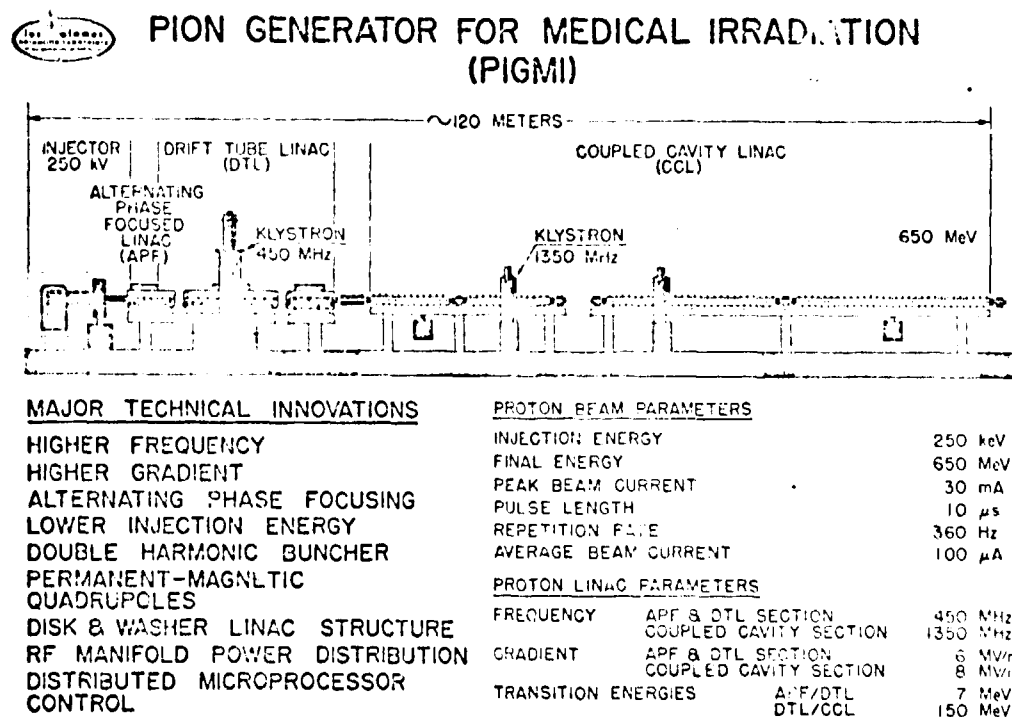


Fig. 11 Characteristics of a dedicated medical pion generator being designed at LASL.